

Numerical Methods to Compute the Coriolis Matrix and Christoffel Symbols for Rigid-Body Systems

Sebastian Echeandia

Aerospace and Mechanical Engineering
University of Notre Dame
Notre Dame, Indiana, 46556

Patrick M. Wensing*

Assistant Professor
Aerospace and Mechanical Engineering
University of Notre Dame
Notre Dame, Indiana, 46556
Email: pwensing@nd.edu

The growth of model-based control strategies for robotics platforms has led to the need for additional rigid-body-dynamics algorithms to support their operation. Toward addressing this need, this article summarizes efficient numerical methods to compute the Coriolis matrix and underlying Christoffel Symbols (of the first kind) for tree-structure rigid-body systems. The resulting algorithms can be executed purely numerically, without requiring any partial derivatives that would be required in symbolic techniques that do not scale. Properties of the presented algorithms share recursive structure in common with classical methods such as the Composite-Rigid-Body Algorithm. The algorithms presented are of the lowest possible order: $O(Nd)$ for the Coriolis Matrix and $O(Nd^2)$ for the Christoffel symbols, where N is the number of bodies and d is the depth of the kinematic tree. A method of order $O(Nd)$ is also provided to compute the time derivative of the mass matrix. A numerical implementation of these algorithms in C/C++ is benchmarked showing computation times on the order of 10-20 μ s for the computation of \mathbf{C} and 40 – 120 μ s for the computation of the Christoffel symbols for systems with 20 degrees of freedom. These results demonstrate feasibility for the adoption of these numerical methods within control loops that need to operate at 1kHz rates or higher, as is commonly required for model-based control applications.

1 Introduction

Rigid-body dynamics algorithms have evolved to be an important component of many model-based robot control strategies. Most commonly, algorithms focus on computing the inverse dynamics of a mechanism, or the components of the equations of motion [1, 2] (e.g., the mass matrix, generalized Coriolis force, generalized gravity force,

etc.) as a precursor to selecting joint torques that achieve desired movements or force-based interactions through contact. These efficient numerical algorithms have seen applications from computed torque control of manipulators to optimization-based whole-body control of legged robots and virtual characters [3–6]. More recently, interest has increased on computing other components of the equations of motion for application in disturbance observer problems [7, 8] or the calculation of partial derivatives for application to gradient-based motion optimization [9–14].

This paper derives a new algorithm for the calculation of the Coriolis matrix that is simple, of lowest order, and has conceptual connection to well-established algorithms for the mass matrix [1, 2]. The algorithm builds from formula that have been provided within the adaptive control community [15–17]. From this Coriolis matrix algorithm, we also derive a new method for the calculation of the Christoffel symbols of the first kind, without requiring any symbolic partial derivatives in the algorithm itself. A related algorithm was recently proposed in [18] that is applicable for kinematic chains with revolute joints. By adopting a coordinate-free development, the work herein is more general (e.g., enabling application to branched systems with prismatic joints, or combinations of prismatic and revolute joints, etc.). Overall, the numeric availability of the Christoffel symbols could have relevance for geometric control algorithms, the calculation of second-order partial derivatives of the inverse dynamics model, or in other geometric methods.

The equations of motion of a rigid-body system can be written as

$$\mathbf{H}(\mathbf{q})\ddot{\mathbf{q}} + \mathbf{C}(\mathbf{q}, \dot{\mathbf{q}})\dot{\mathbf{q}} + \mathbf{g}(\mathbf{q}) = \boldsymbol{\tau} \quad (1)$$

where $\mathbf{q} \in \mathbb{R}^n$ are the generalized coordinates, $\mathbf{H}(\mathbf{q}) \in \mathbb{R}^{n \times n}$ is the (symmetric) mass matrix, $\mathbf{C}(\mathbf{q}, \dot{\mathbf{q}}) \in \mathbb{R}^{n \times n}$ a

*Corresponding Author

Coriolis matrix, $\mathbf{g}(\mathbf{q}) \in \mathbb{R}^n$ the generalized gravity force, and $\boldsymbol{\tau} \in \mathbb{R}^n$ the generalized applied force (often simply the vector of actuator torques for a robot with revolute joints). It is well known that there are many possible choices of $\mathbf{C}(\mathbf{q}, \dot{\mathbf{q}})$ that provide the correct dynamics. All possible choices that provide the correct dynamics satisfy $\dot{\mathbf{q}}^\top (\dot{\mathbf{H}}(\mathbf{q}, \dot{\mathbf{q}}) - 2\mathbf{C}(\mathbf{q}, \dot{\mathbf{q}}))\dot{\mathbf{q}} = 0$ [19], while many satisfy

$$\boldsymbol{\eta}^\top \left[\dot{\mathbf{H}}(\mathbf{q}, \dot{\mathbf{q}}) - 2\mathbf{C}(\mathbf{q}, \dot{\mathbf{q}}) \right] \boldsymbol{\eta} = 0 \quad \forall \mathbf{q}, \dot{\mathbf{q}}, \boldsymbol{\eta} \in \mathbb{R}^n \quad (2)$$

One special choice for \mathbf{C} , denoted by \mathbf{C}^\star , which satisfies (2), is given by:

$$\left[\mathbf{C}^\star(\mathbf{q}, \dot{\mathbf{q}}) \right]_{ij} = \sum_k \Gamma_{ijk}(\mathbf{q}) \dot{q}_k \quad , \text{ where} \quad (3)$$

$$\Gamma_{ijk}(\mathbf{q}) = \frac{1}{2} \left[\frac{\partial H_{ij}}{\partial q_k} + \frac{\partial H_{ik}}{\partial q_j} - \frac{\partial H_{jk}}{\partial q_i} \right] \quad (4)$$

are the Christoffel symbols of the first kind [19]. Note that $\Gamma_{ijk} = \Gamma_{ikj}$ due to the symmetry of \mathbf{H} .

Definition 1 (Christoffel-Consistent Coriolis Factorization). *Consider a system with mass matrix $\mathbf{H}(\mathbf{q})$ and a Coriolis matrix $\mathbf{C}^\star(\mathbf{q}, \dot{\mathbf{q}})$ as given in (3). We call $\mathbf{C}^\star(\mathbf{q}, \dot{\mathbf{q}})$ the Christoffel-consistent Coriolis factorization.*

Definition 2 (Valid Coriolis Factorization). *Consider a system and its Christoffel-consistent Coriolis factorization $\mathbf{C}^\star(\mathbf{q}, \dot{\mathbf{q}})$. A matrix valued function $\mathbf{C}(\mathbf{q}, \dot{\mathbf{q}})$ is said to be a valid Coriolis factorization if for all $\mathbf{q}, \dot{\mathbf{q}} \in \mathbb{R}^n$*

$$\mathbf{C}^\star(\mathbf{q}, \dot{\mathbf{q}})\dot{\mathbf{q}} = \mathbf{C}(\mathbf{q}, \dot{\mathbf{q}})\dot{\mathbf{q}}$$

A valid Coriolis factorization is one that gives the correct equations of motion when used in (1). Yet, the additional property (2) is commonly needed in control [20] and contact detection [7, 8], motivating the following stricter definition.

Definition 3 (Admissible Coriolis Factorization). *Consider a system with mass matrix $\mathbf{H}(\mathbf{q})$. A matrix valued function $\mathbf{C}(\mathbf{q}, \dot{\mathbf{q}})$ is said to be an admissible factorization if*

1. $\mathbf{C}(\mathbf{q}, \dot{\mathbf{q}})$ is a valid factorization
2. $\forall \mathbf{q}, \dot{\mathbf{q}} \in \mathbb{R}^n$, $\dot{\mathbf{H}}(\mathbf{q}, \dot{\mathbf{q}}) - 2\mathbf{C}(\mathbf{q}, \dot{\mathbf{q}})$ is skew symmetric.

Despite the fact that the definition for \mathbf{C}^\star in (3) appears in many textbooks on robotics (e.g., [19, 21]), it is challenging to use directly for complex systems, as the symbolic computation of \mathbf{H} becomes burdensome for systems with many DoFs, and likewise the symbolic differentiation of these equations for the calculation of \mathbf{C}^\star is does not scale well. In this paper, we consider tailored numerical methods to compute admissible factorizations \mathbf{C} , the Christoffel-consistent factorization \mathbf{C}^\star , and the Christoffel symbols Γ_{ijk} by taking advantage of the underlying structure of (1) for open-chain rigid-body systems. Since gravity does not affect Coriolis terms, without loss of generality we ignore gravity in the remainder of this paper.

2 Conventions and Notation

We follow the same conventions and notation as in [1] and cover them briefly as a review. We use spatial vector algebra, which is conceptually equivalent to a Lie-theoretic treatment of rigid-body dynamics [22]. An interested reader may see [23] for description of their relationship. Since spatial vectors and linear operators between them are elements of vector spaces, we review vector space fundamentals, then cover their use in rigid-body dynamics modeling.

2.1 Vector Space Fundamentals

Consider two vector spaces \mathcal{V} and \mathcal{W} and denote by $L(\mathcal{V}, \mathcal{W})$ the vector space of linear operators from \mathcal{V} to \mathcal{W} . The dual vector space \mathcal{V}^* is the set of linear functionals on \mathcal{V} , i.e., $\mathcal{V}^* = L(\mathcal{V}, \mathbb{R})$. For any $\mathbf{y} \in \mathcal{V}^*$ and any $\mathbf{x} \in \mathcal{V}$, we denote the evaluation of the functional $\mathbf{y}(\mathbf{x})$ as $\mathbf{y} \bullet \mathbf{x}$. Given any operator $\mathbf{A} \in L(\mathcal{V}, \mathcal{W})$, denote by $\mathbf{A}^* \in L(\mathcal{W}^*, \mathcal{V}^*)$ the adjoint of \mathbf{A} , which is the unique linear operator with

$$\mathbf{z} \bullet [\mathbf{A}\mathbf{x}] = [\mathbf{A}^* \mathbf{z}] \bullet \mathbf{x} \quad \forall \mathbf{z} \in \mathcal{W}^*, \mathbf{x} \in \mathcal{V}$$

In the case when $\mathcal{W} = \mathcal{V}^*$, the operator \mathbf{A} is said to be self-adjoint if $\mathbf{A} = \mathbf{A}^*$. When bases and their associated dual bases are adopted for \mathcal{V} , \mathcal{W} , \mathcal{V}^* , and \mathcal{W}^* , the matrix representation of \mathbf{A}^* coincides with the transpose of the representation of \mathbf{A} , such that the self-adjoint property corresponds to a symmetric matrix representation of the operator.

2.2 Modeling Connectivity

A rigid-body system can be modeled as a set of N_B bodies connected together by a set of joints, each with up to 6 DoFs. The connectivity of these bodies can generally be described by a connectivity graph. Here, we restrict ourselves to the consideration of rigid-body trees and we denote d as the depth of the tree. Bodies are numbered from 1 through N_B such that body i 's predecessor $p(i)$ towards the root is less than i . These parent/child relationships induce a partial order on the set $\{1, \dots, N_B\}$, which is denoted using a binary relation " \preceq ". We say $j \preceq i$ if body j is in the path from body i to the root of the tree. In this case, j is said to be an ancestor of i . If $i \succeq j$ or $j \succeq i$ then we use say i and j are related, and denote this relationship by $i \sim j$.

For any pair of relatives $i \sim j$ we denote $[ij]$ to be shorthand for the body closest to the leaves:

$$[ij] = \begin{cases} i & \text{if } i \succeq j \\ j & \text{o/w.} \end{cases}$$

As a result, for any pair of relatives $i \sim j$, we have

$$\{k : k \succeq i \text{ and } k \succeq j\} = \{k : k \succeq [ij]\}.$$

The $[ij]$ notation is best understood with an example. For the mechanism in Figure 1 when $i = 6$ and $j = 3$, $[ij] = 6$. Similarly, if $i = 2$ and $j = 10$ we have that $[ij] = 10$. In contrast, $[ij]$ is undefined when $i = 9$ and $j = 5$ because these two bodies are not relatives.

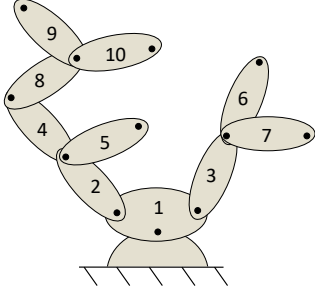


Fig. 1: Connectivity of a Branched Mechanism.

2.3 Spatial Vector Algebra

This section presents an abstract view of spatial vector algebra that will be used to develop algorithms in a coordinate-free manner. Importantly, this perspective will allow us to take derivatives of objects (vectors, inertias, etc.) in a coordinate-free sense, allowing one to dispense with worrying about effects of moving coordinate systems during the derivation of algorithms. Instead, the use of coordinates will be an implementation detail that is easily handled as an after-effect to the main theoretical developments.

Spatial Vectors: The set of all rigid-body motion vectors forms a 6D vector space, denoted \mathcal{M} [1]. Consider a rigid-body moving with spatial velocity $\mathbf{v} \in \mathcal{M}$ and a Cartesian coordinate frame A . We denote the coordinate expression of \mathbf{v} in frame A as

$${}^A\{\mathbf{v}\} = \begin{bmatrix} {}^A\{\boldsymbol{\omega}\} \\ {}^A\{\mathbf{v}_A\} \end{bmatrix}$$

where ${}^A\{\boldsymbol{\omega}\}$ denotes the angular velocity of the body and ${}^A\{\mathbf{v}_A\}$ the linear velocity of the body-fixed point at the origin of A , both expressed using the Cartesian basis of A . Throughout, curly brackets $\{\cdot\}$ will denote the expression of a vector in coordinates for a basis, with the pre-pended superscript (e.g., ${}^A\{\cdot\}$) indicating the basis used.

Suppose that body i and its predecessor $p(i)$ are connected by a d_i degree of freedom (DoF) joint with joint rates $\dot{\mathbf{q}}_i \in \mathbb{R}^{d_i}$. Then, the spatial velocities of these successive bodies are related by

$$\mathbf{v}_i = \mathbf{v}_{p(i)} + \boldsymbol{\Phi}_i \dot{\mathbf{q}}_i \quad (5)$$

where $\mathbf{v}_i, \mathbf{v}_{p(i)} \in \mathcal{M}$ represent the spatial velocities of bodies i and $p(i)$, and $\boldsymbol{\Phi}_i \in L(\mathbb{R}^{d_i}, \mathcal{M})$ maps joint rates to joint velocities. Collecting the configuration of each of the joints, the generalized coordinates are chosen as

$$\mathbf{q} = [\mathbf{q}_1^\top, \dots, \mathbf{q}_{N_B}^\top]^\top. \quad (6)$$

Spatial force vectors (i.e., force/moment pairs) are dual to spatial motion vectors, such that the 6D vector space of spatial forces \mathcal{F} is identified with \mathcal{M}^* . For any motion vector $\mathbf{v} \in \mathcal{M}$ and force vector $\mathbf{f} \in \mathcal{F}$ the ‘‘dot product’’ $\mathbf{v} \bullet \mathbf{f}$ gives the power of a force \mathbf{f} applied at velocity \mathbf{v} .

Spatial inertias are elements of $L(\mathcal{M}, \mathcal{F})$ since they

map motion vectors to force vectors. Yet, since inertias can be linearly parameterized by 10 inertial parameters, inertias reside in a 10-dimensional subspace $\mathcal{I} \subset L(\mathcal{M}, \mathcal{F})$. All inertias are self adjoint, as their expression in coordinates, given in the Appendix, is symmetric [1].

Spatial Equation of Motion: The spatial equation of motion for each body is given compactly by

$$\mathbf{f}_i = \mathbf{I}_i \mathbf{a}_i + \mathbf{v}_i \times^* \mathbf{I}_i \mathbf{v}_i \quad (7)$$

where $\mathbf{f}_i \in \mathcal{F}$ is the net spatial force on body i , $\mathbf{v}_i \in \mathcal{M}$ is body i 's spatial velocity, $\mathbf{a}_i \in \mathcal{M}$ its spatial acceleration, $\mathbf{I}_i \in \mathcal{I}$ its spatial inertia, and $\times^* : \mathcal{M} \times \mathcal{F} \rightarrow \mathcal{F}$ the bilinear cross-product operator between spatial motion vectors and spatial force vectors [1]. From an intuitive standpoint, the cross product $\mathbf{v} \times^* \mathbf{f}$ gives the rate of change in \mathbf{f} when any force field representing it moves with spatial velocity \mathbf{v} . (An expression of this operation in coordinates is given in the Appendix.) This spatial cross-product generalizes the Cartesian formula $\dot{\mathbf{r}} = \boldsymbol{\omega} \times \mathbf{r}$ that describes the rate of change in a 3D vector \mathbf{r} when rotating with angular velocity $\boldsymbol{\omega}$. Note that equation (7) holds in coordinates when any basis is chosen for \mathcal{M} and \mathcal{F} , and in particular it holds even when a frame away from the center of mass is used.

Cross Products: Given any spatial velocity $\mathbf{v} \in \mathcal{M}$, the previous cross product can be used to define a unique linear operator $(\mathbf{v} \times^*) \in L(\mathcal{F}, \mathcal{F})$ such that $(\mathbf{v} \times^*) \mathbf{f} = \mathbf{v} \times^* \mathbf{f}$ for any force vector \mathbf{f} . We swap the order of the cross product arguments and denote $(\mathbf{f} \bar{\times}^*) \in L(\mathcal{M}, \mathcal{F})$ as the unique linear operator satisfying:

$$(\mathbf{f} \bar{\times}^*) \mathbf{v} = (\mathbf{v} \times^*) \mathbf{f} \quad (8)$$

Finally, we denote $(\mathbf{v} \times) \in L(\mathcal{M}, \mathcal{M})$ as the spatial motion/motion cross product defined from the adjoint of $(\mathbf{v} \times^*)$ according to $(\mathbf{v} \times) = -(\mathbf{v} \times^*)^*$. That is, for any $\mathbf{v}, \mathbf{w} \in \mathcal{M}$ and $\mathbf{f} \in \mathcal{F}$

$$[(\mathbf{v} \times) \mathbf{w}] \bullet \mathbf{f} = \mathbf{w} \bullet [-(\mathbf{v} \times^*) \mathbf{f}] \quad (9)$$

Since the adjoint corresponds to a transpose when working in coordinates, for any linear operator \mathbf{A} , we hereafter adopt \mathbf{A}^\top in place of \mathbf{A}^* as a matter of notation.

Factorization of the Spatial Equation: The bi-linear velocity-product term $\mathbf{v}_i \times^* \mathbf{I}_i \mathbf{v}_i$ in (7) can be factorized in a variety of ways to take the form

$$\mathbf{f}_i = \mathbf{I}_i \mathbf{a}_i + \mathbf{B}(\mathbf{v}_i, \mathbf{I}_i) \mathbf{v}_i, \quad (10)$$

where $\mathbf{B}(\mathbf{I}_i, \mathbf{v}_i) \in L(\mathcal{M}, \mathcal{F})$. Note that since $\mathcal{M}^* = \mathcal{F}$ and $\mathcal{F}^* = \mathcal{M}$, it follows that $\mathbf{B}(\mathbf{I}_i, \mathbf{v}_i)^\top \in L(\mathcal{M}, \mathcal{F})$ as well. One immediate factorization can be taken as

$$\mathbf{B}(\mathbf{v}_i, \mathbf{I}_i) = (\mathbf{v}_i \times^*) \mathbf{I}_i \quad (11)$$

while another proposed by Niemeyer and Slotine [24] is:

$$\mathbf{B}(\mathbf{v}_i, \mathbf{I}_i) = \frac{1}{2} ((\mathbf{v}_i \times^*) \mathbf{I}_i + (\mathbf{I}_i \mathbf{v}_i \bar{\times}^*) - \mathbf{I}_i (\mathbf{v}_i \times)) \quad (12)$$

Viewing $\mathbf{B}(\cdot, \cdot)$ as a function from $\mathcal{M} \times \mathcal{I}$ to $L(\mathcal{M}, \mathcal{F})$, the definitions above are bi-linear in their arguments.

Both of these factorizations of the velocity-product terms $\mathbf{B}(\mathbf{v}_i, \mathbf{I}_i) \mathbf{v}_i$ have additional properties that will be of interest for factorization of system-level Coriolis terms $\mathbf{C}(\mathbf{q}, \dot{\mathbf{q}}) \dot{\mathbf{q}}$. We note that the rate of change of the spatial inertia of a body i is given by [1]

$$\dot{\mathbf{I}}_i = [(\mathbf{v}_i \times^*) \mathbf{I}_i - \mathbf{I}_i (\mathbf{v}_i \times)] \in \mathcal{I} \quad (13)$$

This derivative is the derivative of the inertia viewed as an object in the vector space \mathcal{I} , and not the derivative of a matrix in any particular choice of coordinates. Letting $\mathbf{B}_i = \mathbf{B}(\mathbf{v}_i, \mathbf{I}_i)$, we note that for any $\mathbf{v} \in \mathcal{M}$ both of the factorizations, (11) and (12), satisfy

$$\mathbf{v} \bullet \left[(\dot{\mathbf{I}}_i - 2\mathbf{B}_i) \mathbf{v} \right] = 0$$

which is equivalent to the condition that the matrix representation of $\dot{\mathbf{I}}_i - 2\mathbf{B}_i$ is skew-symmetric when expressed in coordinates or equivalently that

$$\dot{\mathbf{I}}_i = \mathbf{B}_i + \mathbf{B}_i^\top. \quad (14)$$

Definition 4 (Admissible Body-Level Factorization). *Any function $\mathbf{B}(\cdot, \cdot) : \mathcal{M} \times \mathcal{I} \rightarrow L(\mathcal{M}, \mathcal{F})$ is said to be an admissible body-level factorization if for all $\mathbf{v} \in \mathcal{M}$, all $\mathbf{I} \in \mathcal{I}$*

1. $\mathbf{B}(\mathbf{v}, \mathbf{I}) \mathbf{v} = \mathbf{v} \times^* (\mathbf{I} \mathbf{v})$ and
2. $(\mathbf{v} \times^*) \mathbf{I} - \mathbf{I} (\mathbf{v} \times) = \mathbf{B}(\mathbf{v}, \mathbf{I}) + \mathbf{B}(\mathbf{v}, \mathbf{I})^\top$

As you might suspect, factorizations of velocity-product terms satisfying this property at a body-by-body level will naturally lead to system-level Coriolis factorizations \mathbf{C} satisfying the analogous property $\dot{\mathbf{H}} - 2\mathbf{C}$ skew symmetric.

3 A Numerical Method for Computing \mathbf{C}

This section presents a new numerical method to compute the Coriolis matrix \mathbf{C} . To the best of the authors' knowledge Niemeyer and Slotine [24–26] (1988) were the first to establish a link between the factorization of body-level velocity-product terms in the Recursive-Newton-Euler Algorithm (RNEA) and the resulting admissibility of a corresponding Coriolis factorization. Lin et al. [15] (1995) were the first to provide general conditions on body-level factorizations that result in admissible \mathbf{C} . Others have taken similar strategies [7, 16, 17, 27] for problems in sensorless contact detection, passivity-based control, or adaptive control. Notably, DeLuca and Ferrajoli [7] are the only to provide an algorithm to compute \mathbf{C} directly, and they do so through N calls to a modified Recursive-Newton Euler

scheme, with total complexity $O(N^2)$ to compute \mathbf{C} . We instead use our coordinate free approach to go one step further and reduce the computation down to $O(Nd)$ through a tailored numerical method for \mathbf{C} , and provide a variant that can compute \mathbf{C}^\star . This later variant is the key to the new Christoffel symbol algorithm in the subsequent section.

3.1 Factoring the RNEA

The RNEA computes the inverse dynamics of a system through two algorithmic sweeps over its kinematic connectivity tree. The first sweep moves outward from base to tips and computes the spatial velocity and acceleration of each body through a recursive implementation of

$$\mathbf{v}_i = \sum_{j \preceq i} \Phi_j \dot{\mathbf{q}}_j \quad (15)$$

$$\mathbf{a}_i = \sum_{j \preceq i} \Phi_j \ddot{\mathbf{q}}_j + \dot{\Phi}_j \dot{\mathbf{q}}_j \quad (16)$$

where $\dot{\Phi}_j = (\mathbf{v}_j \times) \Phi_j + \dot{\Phi}_i$, with $(\mathbf{v}_j \times) \Phi_j$ the derivative due to the joint moving, and $\dot{\Phi}_i$ the derivative due to the axes changing in local coordinates defined by:

$${}^j \left\{ \dot{\Phi}_j \right\} = \frac{d}{dt} {}^j \left\{ \Phi_j \right\} \quad (17)$$

For the case of common revolute joints with axes fixed in local coordinates $\dot{\Phi}_j = \mathbf{0}$.

With this information, the net inertial force required on each body can be computed using (7). A backwards pass of the RNEA sums up these inertial forces over descendants, computing required torques as:

$$\boldsymbol{\tau}_i = \Phi_i^\top \sum_{k \succeq i} \mathbf{f}_k = \Phi_i^\top \sum_{k \succeq i} [\mathbf{I}_k \mathbf{a}_k + \mathbf{v}_k \times^* \mathbf{I}_k \mathbf{v}_k] \quad (18)$$

Using (15) and (16) and Lemma 1 in the Appendix, we can rewrite each torque from (18) as:

$$\boldsymbol{\tau}_i = \sum_{j \sim i} \Phi_i^\top \mathbf{I}_{[ij]}^C \Phi_j \ddot{\mathbf{q}}_j + \left(\Phi_i^\top \mathbf{I}_{[ij]}^C \dot{\Phi}_j + \Phi_i^\top \mathbf{B}_{[ij]}^C \Phi_j \right) \dot{\mathbf{q}}_j \quad (19)$$

where the composite quantities are defined as

$$\mathbf{I}_{[ij]}^C = \sum_{k \succeq [ij]} \mathbf{I}_k \quad (20)$$

$$\mathbf{B}_{[ij]}^C = \sum_{k \succeq [ij]} \mathbf{B}_k(\mathbf{v}_k, \mathbf{I}_k) \quad (21)$$

Detailed derivation is given in the Appendix. Note that \mathbf{I}_j^C has a clear physical interpretation of representing the total inertia of all bodies in the subtree rooted at body j (i.e., body j and all its descendants). Given that there are many possible body-level factorizations, a physical interpretation for \mathbf{B}_j^C is

difficult to provide precisely, however, it suffices to say that it accounts for Coriolis and centripetal forces for body j and all of its descendants. Toward simplifying these expressions, when $i \preceq j$

$$\mathbf{H}_{ij} = \dot{\Phi}_i^\top \mathbf{I}_j^C \Phi_j, \quad (22)$$

$$\mathbf{C}_{ij} = \dot{\Phi}_i^\top (\mathbf{I}_j^C \dot{\Phi}_j + \mathbf{B}_j^C \Phi_j), \quad \text{and} \quad (23)$$

$$(\mathbf{C}_{ji})^\top = \dot{\Phi}_i^\top \mathbf{I}_j^C \Phi_j + \dot{\Phi}_i^\top (\mathbf{B}_j^C)^\top \Phi_j. \quad (24)$$

3.2 Recursive Algorithm for Computing \mathbf{C}

These equations lend themselves to efficient recursive implementation. Let:

$$\mathbf{F}_{1,j} = \mathbf{I}_j^C \dot{\Phi}_j + \mathbf{B}_j^C \Phi_j \quad (25)$$

$$\mathbf{F}_{2,j} = \mathbf{I}_j^C \Phi_j \quad (26)$$

$$\mathbf{F}_{3,j} = (\mathbf{B}_j^C)^\top \Phi_j \quad (27)$$

All of these terms can be computed in $O(N)$ time, since all of \mathbf{I}_j^C and \mathbf{B}_j^C can be computed in $O(N)$ time via summing backward along the tree. Considering body j , for all $O(d)$ ancestors $i \preceq j$:

$$\mathbf{H}_{ij} = \dot{\Phi}_i^\top \mathbf{F}_{2,j} \quad (28)$$

$$\mathbf{C}_{ij} = \dot{\Phi}_i^\top \mathbf{F}_{1,j} \quad (29)$$

$$\mathbf{C}_{ji} = \left(\dot{\Phi}_i^\top \mathbf{F}_{2,j} + \dot{\Phi}_i^\top \mathbf{F}_{3,j} \right)^\top \quad (30)$$

These equations enable an $O(Nd)$ algorithm to compute \mathbf{C} together with \mathbf{H} as given in Algorithm 1. Note that since the algorithm is intended to be run on a computer, vectors and matrices inside are to be expressed in coordinates. The algorithm takes the conventional approach of expressing all quantities in local coordinate frames [1], and transforms the coordinate expression of these vectors through the spatial transformation matrices ${}^i\mathbf{X}_{p(i)}$. For example, when motion vectors are expressed in local coordinates (5) takes the form

$${}^i\{\mathbf{v}_i\} = {}^i\mathbf{X}_{p(i)}{}^{p(i)}\{\mathbf{v}_{p(i)}\} + {}^i\{\dot{\Phi}_i\}\dot{\mathbf{q}}_i$$

such that the matrix ${}^i\mathbf{X}_{p(i)}$ changes the basis of a motion vector from a basis associated with the frame attached to body $p(i)$ to the basis associated with the frame attached to body i . Likewise, the matrix ${}^i\mathbf{X}_{p(i)}^\top$ provides a change of basis for spatial force vectors from frame i to frame $p(i)$, i.e., in the opposite direction as ${}^i\mathbf{X}_{p(i)}$. Finally, for any operator $\mathbf{I} \in \mathcal{M} \rightarrow \mathcal{F}$, the congruence transform ${}^{p(i)}\{\mathbf{I}\} = {}^i\mathbf{X}_{p(i)}^\top {}^i\{\mathbf{I}\} {}^i\mathbf{X}_{p(i)}$ changes the matrix representation of this operator from frame i to frame $p(i)$. While this congruence transform is frequently used to add inertias expressed in different frames [1], it likewise provides the transformation law for the body-level factorization terms \mathbf{B}_i and their associated composite quantities \mathbf{B}_i^C . For cleanliness of presentation, the bracket notation $\{\cdot\}$ and specification of frames are omitted in the algorithm.

The structure of Algorithm 1 is as follows. A for-

Algorithm 1 Coriolis Matrix Algorithm

Require: $\mathbf{q}, \dot{\mathbf{q}}, model$

```

1:  $\mathbf{v}_0 = \mathbf{0}$ 
2: for  $i = 1$  to  $N$  do
3:    $\mathbf{v}_i = {}^i\mathbf{X}_{p(i)}\mathbf{v}_{p(i)} + \dot{\Phi}_i\dot{\mathbf{q}}_i$ 
4:    $\dot{\Phi}_i = (\mathbf{v}_i \times)\Phi_i + \dot{\Phi}_i$ 
5:    $\mathbf{I}_i^C = \mathbf{I}_i$ 
6:    $\mathbf{B}_i^C = \frac{1}{2}[(\mathbf{v}_i \times^*)\mathbf{I}_i + (\mathbf{I}_i\mathbf{v}_i)\bar{\times}^* - \mathbf{I}_i(\mathbf{v}_i \times)]$ 
7: end for
8: for  $j = N$  to  $1$  do
9:    $\mathbf{F}_1 = \mathbf{I}_j^C \dot{\Phi}_j + \mathbf{B}_j^C \Phi_j$ 
10:   $\mathbf{F}_2 = \mathbf{I}_j^C \Phi_j$ 
11:   $\mathbf{F}_3 = (\mathbf{B}_j^C)^\top \Phi_j$ 
12:   $\mathbf{C}_{jj} = \dot{\Phi}_j^\top \mathbf{F}_1$ 
13:   $i = j$ 
14:  while  $i > 0$  do
15:     $\mathbf{F}_1 = {}^i\mathbf{X}_{p(i)}^\top \mathbf{F}_1; \mathbf{F}_2 = {}^i\mathbf{X}_{p(i)}^\top \mathbf{F}_2; \mathbf{F}_3 =$ 
       ${}^i\mathbf{X}_{p(i)}^\top \mathbf{F}_3;$ 
16:     $i = p(i)$ 
17:     $\mathbf{C}_{ij} = \dot{\Phi}_i^\top \mathbf{F}_1$ 
18:     $\mathbf{C}_{ji} = (\dot{\Phi}_i^\top \mathbf{F}_2 + \dot{\Phi}_i^\top \mathbf{F}_3)^\top$ 
19:     $\mathbf{H}_{ij} = (\mathbf{H}_{ji})^\top = \dot{\Phi}_i^\top \mathbf{F}_2$ 
20:     $\dot{\mathbf{H}}_{ij} = (\dot{\mathbf{H}}_{ji})^\top = \dot{\Phi}_i^\top \mathbf{F}_2 + \dot{\Phi}_i^\top (\mathbf{F}_1 + \mathbf{F}_3)$ 
21:  end while
22:   $\mathbf{I}_{p(j)}^C = \mathbf{I}_{p(j)}^C + {}^j\mathbf{X}_{p(j)}^\top \mathbf{I}_j^C {}^j\mathbf{X}_{p(j)}$ 
23:   $\mathbf{B}_{p(j)}^C = \mathbf{B}_{p(j)}^C + {}^j\mathbf{X}_{p(j)}^\top \mathbf{B}_j^C {}^j\mathbf{X}_{p(j)}$ 
24: end for
25: return  $\mathbf{H}, \dot{\mathbf{H}}, \mathbf{C}$ 
```

ward sweep (lines 2-7) computes the velocity of the bodies throughout the kinematic tree as well as the initial composite terms \mathbf{I}_i^C and \mathbf{B}_i^C . Other valid body-level factorizations may be used on line 6. The backward sweeps (lines 8-24) compute the entries of the Coriolis and mass matrices. Lines 22 and 23 are the propagation of the composite terms towards the root of the tree. The while loop (lines 14-21) computes the entries for \mathbf{H} , $\dot{\mathbf{H}}$, and \mathbf{C} associated with body j and propagates the computation down to all its predecessors. Overall, the algorithm has complexity $O(Nd)$, and its correctness is justified through the following proposition.

Proposition 1 (Algorithm for an Admissible Coriolis Factorization). *Suppose that Algorithm 1 uses an admissible body-level factorization $\mathbf{B}(\mathbf{v}, \mathbf{I})$ on Line 6. Then, the resulting $\mathbf{C}(\mathbf{q}, \dot{\mathbf{q}})$ from Algorithm 1 is an admissible Coriolis factorization.*

Proof. (Mirroring [15]) To show that the algorithm produces an admissible factorization for \mathbf{C} , it remains to show that $\dot{\mathbf{H}} = \mathbf{C} + \mathbf{C}^\top$. Note that

$$\dot{\mathbf{H}}_{ij} = \dot{\Phi}_i^\top \mathbf{I}_j^C \Phi_j + \dot{\Phi}_i^\top \left(\dot{\mathbf{I}}_j^C \Phi_j + \mathbf{I}_j^C \dot{\Phi}_j \right)$$

Yet, if an admissible body-level factorization is employed, (14) holds and also implies that $\dot{\mathbf{I}}_j^C = \mathbf{B}_j^C + (\mathbf{B}_j^C)^\top$. It then follows that

$$\dot{\mathbf{H}}_{ij} = \dot{\Phi}_i^\top (\mathbf{F}_1 + \mathbf{F}_3) + \dot{\Phi}_i^\top \mathbf{F}_2$$

Thus, the result of Algorithm 1 provides $\dot{\mathbf{H}} = \mathbf{C} + \mathbf{C}^\top$. \square

Proposition 2 (Algorithm for the Christoffel-Consistent Factorization). *Suppose that the algorithm uses the body-level factorization from (12) as given on Line 6. Suppose that each joint is a single DoF and each joint model satisfies $\dot{\Phi}_i = \mathbf{0}$. Then, Algorithm 1 provides the Christoffel-consistent factorization \mathbf{C}^\star .*

Proof. See Section 3.3 of [26] for the case of an unbranched tree. Correctness with branching generalizes immediately by replacing integer ordering $i \leq j$ with the partial order $i \preceq j$ due to branching. \square

Remark 1. *Note that [26] provides an algorithm to compute $\mathbf{C}^\star(\mathbf{q}, \dot{\mathbf{q}})\dot{\mathbf{q}}_r$ where $\dot{\mathbf{q}}_r \in \mathbb{R}^n$ is a reference joint velocity not necessarily equal to $\dot{\mathbf{q}}$. While we rely on their theoretical result in our proof, our ability to compute \mathbf{C}^\star itself distinguishes this work from [26].*

3.3 Changes of Generalized Coordinates

The algorithm presented only applies when the generalized coordinates are chosen as the collection of joint variables (6). If other generalized coordinates are desired, a change of coordinates can be applied to the output of Algorithm 1. Let $\bar{\mathbf{q}}$ represent a different choice of generalized coordinates with

$$\mathbf{A} = \frac{\partial \mathbf{q}}{\partial \bar{\mathbf{q}}} \quad \text{such that} \quad A_{ij} = \frac{\partial q_i}{\partial \bar{q}_j} \quad (31)$$

Using $\dot{\mathbf{q}} = \mathbf{A}\dot{\bar{\mathbf{q}}}$ and $\ddot{\mathbf{q}} = \mathbf{A}\ddot{\bar{\mathbf{q}}} + \dot{\mathbf{A}}\dot{\bar{\mathbf{q}}}$ in (1), and multiplying both sides by \mathbf{A}^\top , it follows that:

$$\bar{\mathbf{H}} = \mathbf{A}^\top \mathbf{H} \mathbf{A} \quad (32)$$

$$\bar{\mathbf{C}} = \mathbf{A}^\top \mathbf{C} \mathbf{A} + \mathbf{A}^\top \dot{\mathbf{H}} \mathbf{A} \quad (33)$$

$$\bar{\mathbf{g}} = \mathbf{A}^\top \mathbf{g} \quad (34)$$

$$\bar{\boldsymbol{\tau}} = \mathbf{A}^\top \boldsymbol{\tau} \quad (35)$$

leads to a valid set of transformed equations of motion

$$\bar{\mathbf{H}}\ddot{\bar{\mathbf{q}}} + \bar{\mathbf{C}}\dot{\bar{\mathbf{q}}} + \bar{\mathbf{g}} = \bar{\boldsymbol{\tau}} \quad (36)$$

Proposition 3 (Admissible Factorization Under a Change of Coordinates [15]). *If the matrix $\mathbf{C}(\mathbf{q}, \dot{\mathbf{q}})$ is an admissible factorization in the coordinates \mathbf{q} , then $\bar{\mathbf{C}}(\bar{\mathbf{q}}, \dot{\bar{\mathbf{q}}})$ given by (33) is an admissible factorization for the coordinates $\bar{\mathbf{q}}$.*

Proof. (Via [15]) The derivation for $\bar{\mathbf{C}}$ shows that it provides proper equations of motion, thus it is a valid factorization. Since \mathbf{C} is an admissible factorization $\dot{\mathbf{H}} = \mathbf{C} + \mathbf{C}^\top$.

Considering the derivative of $\bar{\mathbf{H}}$ from (32),

$$\begin{aligned} \dot{\bar{\mathbf{H}}} &= \dot{\mathbf{A}}^\top \mathbf{H} \mathbf{A} + \mathbf{A}^\top \dot{\mathbf{H}} \mathbf{A} + \mathbf{A}^\top \dot{\mathbf{H}} \mathbf{A} \\ &= \dot{\mathbf{A}}^\top \mathbf{H} \mathbf{A} + \mathbf{A}^\top (\mathbf{C} + \mathbf{C}^\top) \mathbf{A} + \mathbf{A}^\top \dot{\mathbf{H}} \mathbf{A} \\ &= \bar{\mathbf{C}}^\top + \bar{\mathbf{C}} \end{aligned}$$

\square

A remarkable property of this transformation law (33) is that it transforms the unique Christoffel-consistent factorization in one set of coordinates to the unique Christoffel-consistent factorization in the transformed coordinates.

Theorem 1 (Christoffel-Consistent Factorization Under A Change of Coordinates). *Suppose $\mathbf{C}^\star(\mathbf{q}, \dot{\mathbf{q}})$ is the unique factorization given by the Christoffel symbols in the coordinates \mathbf{q} via (3). Consider a change of coordinates to $\bar{\mathbf{q}}$ with \mathbf{A} defined as in (31). Then, the unique Coriolis factorization given by the Christoffel symbols in the coordinates $\bar{\mathbf{q}}$ is*

$$\bar{\mathbf{C}}^\star = \mathbf{A}^\top \mathbf{C}^\star \mathbf{A} + \mathbf{A}^\top \dot{\mathbf{H}} \mathbf{A} \quad (37)$$

Proof. See Appendix. \square

3.4 Remarks

Remark 2. *Due to the symmetry of the Christoffel symbols, any valid factorization $\mathbf{C}(\mathbf{q}, \dot{\mathbf{q}})$ can be used to determine \mathbf{C}^\star via*

$$\mathbf{C}^\star(\mathbf{q}, \dot{\mathbf{q}}) = \frac{1}{2} \frac{\partial}{\partial \dot{\mathbf{q}}} [\mathbf{C}(\mathbf{q}, \dot{\mathbf{q}})\dot{\mathbf{q}}] \quad (38)$$

Of course, using this result requires knowledge of the symbolic form of $\mathbf{C}(\mathbf{q}, \dot{\mathbf{q}})\dot{\mathbf{q}}$, whereas, Algorithm 1 can be used to compute \mathbf{C}^\star numerically at any $\mathbf{q}, \dot{\mathbf{q}}$ in accordance with Proposition 2. In this sense, the algorithm to compute \mathbf{C}^\star also provides an efficient method to compute the partial derivatives of Inverse Dynamics w.r.t. $\dot{\mathbf{q}}$. Likewise, existing algorithms for computing these partials can be straightforwardly modified to calculate \mathbf{C}^\star (i.e., by considering the factor of $\frac{1}{2}$ in (38)).

Remark 3. *The results relating the body-level factorization of the velocity-product terms to admissible Coriolis matrices also has applicability for alternate methods of computing the Coriolis matrix. An alternate form of (18) can be considered from the body Jacobians $\mathbf{J}_i \in L(\mathbb{R}^N, \mathcal{M})$ such that each body velocity satisfies $\mathbf{v}_i = \mathbf{J}_i \dot{\mathbf{q}}_i$. Using these body Jacobians*

$$\boldsymbol{\tau} = \sum_k \mathbf{J}_k^\top (\mathbf{I}_k \mathbf{a}_k + \mathbf{B}(\mathbf{v}_k, \mathbf{I}_k) \mathbf{v}_k)$$

Noting that $\mathbf{a}_i = \mathbf{J}_i \ddot{\mathbf{q}} + \dot{\mathbf{J}}_i \dot{\mathbf{q}}$ it follows that

$$\boldsymbol{\tau} = \sum_k \mathbf{J}_k^\top \mathbf{I}_k \mathbf{J}_k \ddot{\mathbf{q}} + \mathbf{J}_k^\top \left[\mathbf{B}(\mathbf{v}_k, \mathbf{I}_k) \mathbf{J}_k + \mathbf{I}_k \dot{\mathbf{J}}_k \right] \dot{\mathbf{q}}$$

such that the formulas

$$\mathbf{H} = \sum_k \mathbf{J}_k^\top \mathbf{I}_k \mathbf{J}_k \quad (39)$$

$$\mathbf{C} = \sum_k \mathbf{J}_k^\top \left[\mathbf{B}(\mathbf{v}_k, \mathbf{I}_k) \mathbf{J}_k + \mathbf{I}_k \dot{\mathbf{J}}_k \right] \quad (40)$$

can be used to compute \mathbf{H} and \mathbf{C} . This approach is the one taken in, e.g., [28], however, it results in an $O(N_B^3)$ algorithm to compute \mathbf{H} and \mathbf{C} . Herein, each \mathbf{J}_k is a linear mapping to the vector space of spatial velocities, and $\dot{\mathbf{J}}_k$ is the time derivative of this operator. Via comparison, in [28] ${}^k\{\mathbf{J}_k\} \in L(\mathbb{R}^n, \mathbb{R}^6)$ is used, which provides

$${}^k\{\mathbf{v}_k\} = {}^k\{\mathbf{J}_k\} \dot{\mathbf{q}} \quad (41)$$

With $\dot{\mathbf{J}}_k$ the unique operator satisfying ${}^k\{\dot{\mathbf{J}}_k\} = \frac{d}{dt} {}^k\{\mathbf{J}_k\}$:

$$\dot{\mathbf{J}}_k = \dot{\mathbf{J}}_k + (\mathbf{v}_k \times) \mathbf{J}_k$$

and so

$$\mathbf{C} = \sum_k \mathbf{J}_k^\top \left[\mathbf{B}(\mathbf{I}_k, \mathbf{v}_k) \mathbf{J}_k + \mathbf{I}_k \dot{\mathbf{J}}_k + \mathbf{I}_k (\mathbf{v}_k \times) \mathbf{J}_k \right]$$

Remark 4. Note that all of the previous results have required generalized coordinates, whereas rigid-body dynamics can also be derived using generalized speeds (e.g., using Kane's method [29]). Suppose some generalized speeds $\boldsymbol{\nu} \in \mathbb{R}^n$ are used with $\mathbf{A}(\mathbf{q}) = \frac{\partial \dot{\mathbf{q}}}{\partial \boldsymbol{\nu}}$. Using (32)-(35) with this choice of \mathbf{A} leads to a valid set of transformed equations of motion, and the proof strategy of Proposition 3 generalizes such that $\dot{\mathbf{H}} = \overline{\mathbf{C}} + \overline{\mathbf{C}}^\top$ still holds. If one redefines \mathbf{J}_k such that $\mathbf{v}_k = \mathbf{J}_k \boldsymbol{\nu}$, then (40) can also be used to derive an admissible Coriolis factorization from an admissible body-level factorization when using generalized speeds.

Remark 5. The use of generalized speeds is popular, e.g., in floating-base systems such as humanoid robots [30] or quadrotors [31] where the angular velocity of a main body is included in the generalized speeds. This choice is often adopted to avoid singularities associated with Euler angles or other three-parameter representations of orientation. In these systems, the use of the CoM position in the generalized coordinates leads to decoupled equations of motion [30,31]. Consider generalized coordinates $\mathbf{q} = [\mathbf{p}_{CoM}, \mathbf{q}_2]$ where $\mathbf{p}_{CoM} \in \mathbb{R}^3$ gives the CoM position of a free-floating system, and \mathbf{q}_2 is independent of the CoM position. In this case, the mass matrix takes the block-diagonal form [30]

$$\mathbf{H}(\mathbf{q}_2) = \begin{bmatrix} M \mathbf{1}_3 & \mathbf{0} \\ \mathbf{0} & \mathbf{H}_{22}(\mathbf{q}_2) \end{bmatrix}$$

where $M \in \mathbb{R}$ is the total mass of the system. Due to the form of \mathbf{H} , $\Gamma_{ijk} = 0$ whenever i, j, k is 1, 2, or 3. It then

follows that

$$\overline{\mathbf{C}}^\star(\overline{\mathbf{q}}, \dot{\overline{\mathbf{q}}}) = \begin{bmatrix} \mathbf{0} & \mathbf{0} \\ \mathbf{0} & \overline{\mathbf{C}}_{22}^\star(\overline{\mathbf{q}}_2, \dot{\overline{\mathbf{q}}}_2) \end{bmatrix} \quad (42)$$

such that the Christoffel-consistent factorization likewise inherits additional sparsity. Consider generalized speeds chosen as $\boldsymbol{\nu} = [\mathbf{p}_{CoM}^\top, \boldsymbol{\nu}_2^\top]^\top$, where $\boldsymbol{\nu}_2$ is chosen to be independent of the CoM velocity. Then, applying the Coriolis matrix transformation (33) results in an admissible factorization for these generalized speeds with the same sparsity as (42). Alternately, if one uses the body-level factorization in (12) and Jacobians satisfying $\mathbf{v}_k = \mathbf{J}_k \boldsymbol{\nu}$, then (40) directly provides the same Coriolis matrix (without transformation), inheriting the same sparsity as in (42). This sparsity pattern can be used to simplify passivity-based control laws and their analysis [30, 31].

4 Computing Christoffel Symbols

This section builds upon the Coriolis matrix results of the previous section to produce an algorithm for the Christoffel Symbols of the first kind. We consider the case when all joints are a single DoF and $\dot{\Phi}_i = 0$ for all i . In this case, via Proposition 2, the factorization in (12) leads to a \mathbf{C} matrix that is not just admissible, but also coincides with \mathbf{C}^\star [26]. This property implies that

$$\Gamma_{ijk} = \frac{\partial \mathbf{C}_{ij}^\star}{\partial \dot{q}_k}.$$

This section will first derive these partials and develop a recursive algorithm for calculation of all the symbols Γ_{ijk} through partials of \mathbf{C}_{ij}^\star as given in (23) and repeated below

$$\mathbf{C}_{ij}^\star = \Phi_i^\top (\mathbf{I}_j^C \dot{\Phi}_j + \mathbf{B}_j^C \Phi_j) \quad (43)$$

Since the formula for \mathbf{C}_{ij}^\star in (43) includes effects from velocities \mathbf{v} , rates of change in joint axes $\dot{\Phi}$, and body-level factorizations \mathbf{B} , the derivation proceeds to consider partials of each of these terms before combining them together. Considering the spatial velocity of a body from (15), it follows that

$$\frac{\partial \mathbf{v}_j}{\partial \dot{q}_k} = \begin{cases} \Phi_k & \text{if } j \succeq k \\ \mathbf{0} & \text{o/w.} \end{cases} \quad (44)$$

Since $\dot{\Phi}_j = \mathbf{v}_j \times \Phi_j$ it then follows similarly that

$$\frac{\partial \dot{\Phi}_j}{\partial \dot{q}_k} = \begin{cases} \Phi_k \times \Phi_j & \text{if } j \succeq k \\ \mathbf{0} & \text{o/w.} \end{cases} \quad (45)$$

Physically, (45) indicates that $\dot{\Phi}_j$ only changes with \dot{q}_k if body j moves with changes to joint k . That is, if body j is part of a chain from body k to the leaves (Fig. 2).

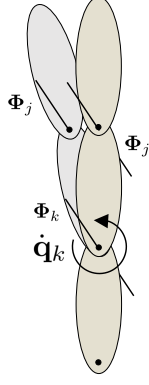


Fig. 2: Depiction of the motion of spatial joint axes due to the joint velocities of their ancestors.

Continuing to consider the partials of the remaining constitutive pieces of (43), recall that:

$$\mathbf{B}_{[ij]}^C = \sum_{\ell \succeq [ij]} \mathbf{B}(\mathbf{v}_\ell, \mathbf{I}_\ell)$$

and $\mathbf{B}(\mathbf{v}_\ell, \mathbf{I}_\ell)$ is bi-linear in its arguments. From this information and (44), it follows that

$$\begin{aligned} \frac{\partial \mathbf{B}_{[ij]}^C}{\partial \dot{q}_k} &= \sum_{\ell \succeq [ij]} \mathbf{B} \left(\frac{\partial \mathbf{v}_\ell}{\partial \dot{q}_k}, \mathbf{I}_\ell \right) \\ &= \sum_{\ell \in \{\ell \succeq [ij] \text{ and } \ell \succeq k\}} \mathbf{B}(\Phi_k, \mathbf{I}_\ell) \\ &= \begin{cases} \mathbf{B}(\Phi_k, \mathbf{I}_{[ijk]}^C) & \text{if } [ij] \sim k \\ \mathbf{0} & \text{o/w} \end{cases} \end{aligned}$$

where $[ijk] = [[ij]k]$ gives the body closest to the leaves for the mutual relatives i, j , and k .

With these elements, we now consider the partial derivative of \mathbf{C} :

$$\Gamma_{ijk} = \frac{\partial \mathbf{C}_{ij}}{\partial \dot{q}_k} = \Phi_i^\top \mathbf{I}_{[ij]}^C \frac{\partial \Phi_j}{\partial \dot{q}_k} + \Phi_i^\top \frac{\partial \mathbf{B}_{[ij]}^C}{\partial \dot{q}_k} \Phi_j$$

Without loss of generality, since $\Gamma_{ijk} = \Gamma_{ikj}$ we consider $j \succeq k$. It then follows that when i, j , and k are mutually related (i.e., $i \sim j$, $j \sim k$, and $i \sim k$) then

$$\Gamma_{ijk} = \Gamma_{ikj} = \Phi_i^\top \mathbf{B}(\Phi_k, \mathbf{I}_{[ijk]}^C) \Phi_j$$

and $\Gamma_{ijk} = \Gamma_{ikj} = 0$ otherwise.

Suppose that $i \preceq j \preceq k$. Then, permuting indices

$$\Gamma_{ijk} = \Gamma_{ikj} = \Phi_i^\top \mathbf{B}(\Phi_k, \mathbf{I}_k^C) \Phi_j \quad (46)$$

$$\Gamma_{jik} = \Gamma_{jki} = \Phi_j^\top \mathbf{B}(\Phi_k, \mathbf{I}_k^C) \Phi_i \quad (47)$$

$$\Gamma_{kij} = \Gamma_{kji} = \Phi_k^\top \mathbf{B}(\Phi_j, \mathbf{I}_k^C) \Phi_i \quad (48)$$

Considering this last identity we have:

$$\Gamma_{kij} = \frac{1}{2} \Phi_k^\top ((\Phi_j \times^*) \mathbf{I}_k^C \Phi_i + (\Phi_i \times^*) \mathbf{I}_k^C \Phi_j - \mathbf{I}_k^C (\Phi_j \times) \Phi_i)$$

Application of the property

$$\mathbf{v}_1^\top (\mathbf{v}_2 \times^*) \mathbf{f} = \mathbf{f}^\top (\mathbf{v}_1 \times) \mathbf{v}_2$$

then provides

$$\Gamma_{kij} = \frac{1}{2} \Phi_i^\top [\mathbf{I}_k^C (\Phi_k \times) - (\Phi_k \times^*) \mathbf{I}_k^C + (\mathbf{I}_k^C \Phi_k \bar{\times}^*)] \Phi_j \quad (49)$$

$$= \Phi_i^\top [(\mathbf{I}_k^C \Phi_k \bar{\times}^*) - \mathbf{B}(\Phi_k, \mathbf{I}_k^C)] \Phi_j \quad (50)$$

To turn these formulas into a recursive algorithm, let

$$\tilde{\mathbf{B}}_k = \mathbf{B}(\Phi_k, \mathbf{I}_k^C)$$

$$\mathbf{D}_k = (\mathbf{I}_k^C \Phi_k \bar{\times}^*) - \tilde{\mathbf{B}}_k$$

these quantities can be computed for all k in $O(N)$ total time, similar to \mathbf{I}_k^C . Working through (46), (47), and (50), we likewise define

$$\mathbf{F}_{1,jk} = \tilde{\mathbf{B}}_k \Phi_j \quad (51)$$

$$\mathbf{F}_{2,jk} = \tilde{\mathbf{B}}_k^\top \Phi_j \quad (52)$$

$$\mathbf{F}_{3,jk} = \mathbf{D}_k \Phi_j \quad (53)$$

which can be computed for all $j \preceq k$ in $O(Nd)$ total time. Finally, these intermediate quantities can be used to compute

$$\Gamma_{ijk} = \Gamma_{ikj} = \Phi_i^\top \mathbf{F}_{1,jk} \quad (54)$$

$$\Gamma_{jik} = \Gamma_{jki} = \Phi_i^\top \mathbf{F}_{2,jk} \quad (55)$$

$$\Gamma_{kij} = \Gamma_{kji} = \Phi_i^\top \mathbf{F}_{3,jk} \quad (56)$$

which can be computed for all $i \preceq j \preceq k$ in $O(Nd^2)$ total time. Algorithm 2 places all of these calculations into coordinates adding in the necessary transformation matrices to complete the algorithm.

In Algorithm 2, the forward sweep (lines 2-4) initializes the composite inertia for each body. Lines 6 and 7 compute $\tilde{\mathbf{B}}$ and \mathbf{D} . The nested while loops (lines 9-20) compute all the entries of Γ_{ijk} . Note that there are two while loops to cover all permutations of indices j and i for a given k . Lines 21 and 22 propagate $\tilde{\mathbf{B}}$ and \mathbf{D} down the tree as the indices change, and line 25 updates the composite inertia term as the algorithm sweeps toward the root of the tree.

Remark 6. It is noted that alternate closed-form expressions for the Christoffel symbols have been given in [22, 32–34] within a Lie group framework and in [35] using spatial vectors. The focus of these previous results has been in providing a closed-form expression, whereas the main contribution of the development here is a recursive algorithm of lowest possible order.

Algorithm 2 Christoffel Symbols Algorithm

Require: $\mathbf{q}, model$

```

1:  $\mathbf{v}_0 = \mathbf{0}$ 
2: for  $i = 1$  to  $N$  do
3:    $\mathbf{I}_i^C = \mathbf{I}_i$ 
4: end for
5: for  $k = N$  to  $1$  do
6:    $\tilde{\mathbf{B}} = \frac{1}{2}[(\Phi_k \times^*)\mathbf{I}_k^C + (\mathbf{I}_k^C \Phi_k) \bar{\times}^* - \mathbf{I}_k^C(\Phi_k \times)]$ 
7:    $\mathbf{D} = (\mathbf{I}_k^C \Phi_k \bar{\times}^*) - \tilde{\mathbf{B}}$ 
8:    $j = k$ 
9:   while  $j > 0$  do
10:     $\mathbf{F}_1 = \tilde{\mathbf{B}} \Phi_j$ 
11:     $\mathbf{F}_2 = \tilde{\mathbf{B}}^\top \Phi_j$ 
12:     $\mathbf{F}_3 = \mathbf{D} \Phi_j$ 
13:     $i = j$ 
14:    while  $i > 0$  do
15:       $\Gamma_{ijk} = \Gamma_{ikj} = \Phi_1^\top \mathbf{F}_1$ 
16:       $\Gamma_{jik} = \Gamma_{jki} = \Phi_1^\top \mathbf{F}_2$ 
17:       $\Gamma_{kji} = \Gamma_{kij} = \Phi_1^\top \mathbf{F}_3$ 
18:       $\mathbf{F}_1 = {}^i \mathbf{X}_{p(i)}^\top \mathbf{F}_1; \mathbf{F}_2 = {}^i \mathbf{X}_{p(i)}^\top \mathbf{F}_2; \mathbf{F}_3 =$ 
 ${}^i \mathbf{X}_{p(i)}^\top \mathbf{F}_3;$ 
19:       $i = p(i)$ 
20:    end while
21:     $\tilde{\mathbf{B}} = {}^j \mathbf{X}_{p(j)}^\top \tilde{\mathbf{B}} {}^j \mathbf{X}_{p(j)}$ 
22:     $\mathbf{D} = {}^j \mathbf{X}_{p(j)}^\top \mathbf{D} {}^j \mathbf{X}_{p(j)}$ 
23:     $j = p(j)$ 
24:  end while
25:   $\mathbf{I}_{p(k)}^C = \mathbf{I}_{p(k)}^C + {}^k \mathbf{X}_{p(k)}^\top \mathbf{I}_k^C {}^k \mathbf{X}_{p(k)}$ 
26: end for
27: return  $\Gamma$ 

```

5 Results

To verify the correctness of our algorithms, we compared our results against those from known algorithms, such as the Recursive Newton-Euler Algorithm (RNEA). From the equations of motion of a rigid-body system, we know that when the gravity force is 0 and $\ddot{\mathbf{q}} = \mathbf{0}$, the torque at each joint is equal to the product of $\mathbf{C}(\mathbf{q}, \dot{\mathbf{q}})$ and $\dot{\mathbf{q}}$. Under those conditions for a serial kinematic chain of 10 degrees of freedom, $\mathbf{C}\dot{\mathbf{q}}$ computed through Algorithm 1 with randomized inputs had a maximum error of only 7.3×10^{-12} compared to the torque computed by the RNEA (Table 1). This check was repeated with 5 and 15 bodies (Table 1), providing similar results and ensuring the validity of the algorithm.

With a verified valid factorization for \mathbf{C} we verified that Algorithm 1 provides an admissible \mathbf{C} by ensuring $\dot{\mathbf{H}} = \mathbf{C} + \mathbf{C}^\top$ when the body-level factorization (12) was used. When using this body-level factorization, more specifically, the outputs of Algorithm 1 and Algorithm 2 are consistent with one another if (3) is satisfied. In both cases the residuals for our calculated values were negligible, which supports the

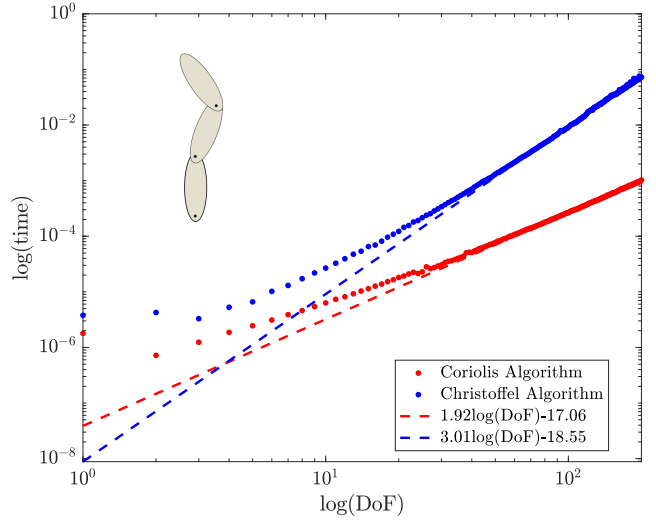


Fig. 3: Performance for Serial Kinematic Chains.

correctness of the proposed algorithms (Table 1).

We implemented Algorithms 1 and 2 in C/C++ using the Rigid-Body Dynamics Library [36]. Both algorithms performed as expected. For serial kinematic chains, the computational cost to compute the Christoffel Symbols scaled approximately as $O(N^3)$ while the cost for the Coriolis Matrix scaled as $O(N^2)$ (Fig. 3). For a branched mechanism with a branching factor of 2, the depth goes as $O(\log N)$, and so the time to compute the Coriolis Matrix should increase as $O(N \log N)$ and that of Christoffel Symbols scales as $O(N(\log N)^2)$ (Fig. 4). A polynomial fit to these log-log plots verifies that the order of the algorithms in this case is above $O(N)$ but below $O(N^2)$, in agreement with the theoretical complexity analysis. The difference between serial and branching mechanisms is due to the branching factor. For a branched mechanism, $d < N$ so that the $O(Nd)$ and $O(Nd^2)$ behaviors grow slower than in the serial case where $d = N$. Accordingly, the algorithms are faster for robotic systems with higher branching factors, like quadrupeds, than other less branched configurations such as bipeds (Fig. 5).

In terms of run time, Algorithms 1 and 2 proved to be fast enough for online control loops that run thousands of times per second. For rigid-body chains of 20 DoFs, the algorithms take approximately 20 μs to numerically evaluate the Coriolis matrix and up to 122 μs to evaluate the Christoffel symbols (Table 2). The longer computation times for the Christoffel symbols are associated with trees that have little to no branching. In contrast, for a 20-DoF kinematic trees with a branching factor of 2 (binary tree), all Γ_{ijk} can be evaluated in as little as 33 μs . These results are particularly promising for the Christoffel symbols algorithm.

The benefits of the algorithm can also be observed compared to when computing Γ_{ijk} symbolically. Commonly, the first step to symbolically compute Γ_{ijk} is to calculate the mass matrix symbolically with an algorithm such as CRBA [1, 2]. Then it is necessary to carry out a large number of partial derivatives of \mathbf{H} via (3) to find the Christoffel

Table 1: Validity Checks for a Serial Kinematic Chain of 5,10, and 15 Degrees of Freedom (Maximum Error)

	$N_B = 5$	$N_B = 10$	$N_B = 15$
$\mathbf{C}\dot{\mathbf{q}} - \boldsymbol{\tau}$ (RNEA)	5.7×10^{-14}	7.3×10^{-12}	2.9×10^{-11}
$\dot{\mathbf{H}} - (\mathbf{C} + \mathbf{C}^\top)$	3.6×10^{-15}	5.7×10^{-14}	2.3×10^{-13}
$\sum_k [\Gamma_{1,1,k}, \dot{q}_k] - \mathbf{C}_{1,1}$	1.1×10^{-13}	7.3×10^{-12}	1.0×10^{-12}

Table 2: Computation Time of Coriolis Matrix and Christoffel Symbols for Common Rigid-Body Systems.

	$\mathbf{C}(\mu s)$	$\Gamma_{ijk}(\mu s)$
Serial Chain (20 DoF)	18	122
Branched Mechanism (20 DoF)	10	33
Biped (20 actuated DoF)	13	64
Quadruped (20 actuated DoF)	10	37

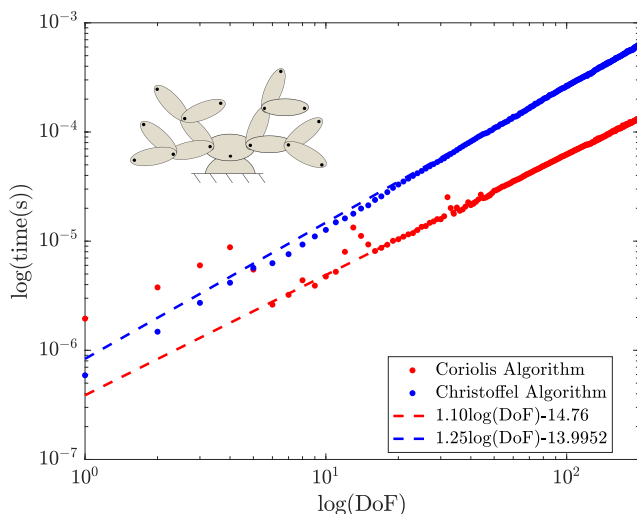


Fig. 4: Performance for Branching Mechanism (Branching Factor of 2).

symbols. These symbolic calculations become very complex for systems with more than just a few bodies. Using symbolic variables in MATLAB, this approach was carried out and timed for planar branched mechanisms (branching factor of 2) with $N_B = 5, 10,$ and 15 bodies. This approach was compared to calling Algorithm 2 with symbolic inputs (Table 3). The two strategies were found roughly comparable, and both are significantly slower than when calling Algorithm 2 with numeric inputs. In this case, if a symbolic result is desired, our algorithm is preferred over the conventional formula requiring partial derivatives, and these benefits increase with additional bodies. In serial chains, it was surprisingly found that symbolically evaluating the partials

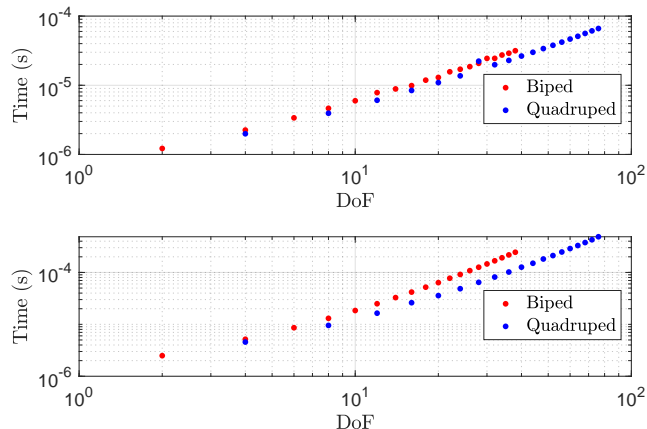


Fig. 5: Computation Cost for Biped and Quadrupeds.

Table 3: Run Time of Different Methods to Symbolically Compute the Christoffel Symbols (Branched Mechanism with Branching Factor of Two).

N_B	5	10	15
Partials of \mathbf{H} (4)	1.23s	7.83s	27.1s
Algorithm 2	0.97s	3.11s	5.88s

of \mathbf{H} as in (3) was preferable to symbolically running Algorithm 2. However, beyond $N_B = 15$, both approaches take on the order of hours to run symbolically, and quickly thereafter are unable to complete within a day. This performance makes the numerical evaluation of the Christoffel symbols more remarkable when considering the results of Table 2. In the time it takes to run Algorithm 2 symbolically for a 10-DoF planar serial chain (26.8 minutes), Algorithm 2 can numerically evaluate all symbols Γ_{ijk} more than 10^7 times.

6 Conclusions

In this paper, we developed computationally efficient algorithms to numerically calculate the Coriolis Matrix and its associated Christoffel Symbols. By choosing a suitable factorization for the spatial equations of motion, we were able to exploit the bi-linearity in \mathbf{v} and \mathbf{I} of the factor $\mathbf{B}(\mathbf{v}_i, \mathbf{I}_i)$ to find a factorization for the system-level Coriolis terms. We found expressions for each entry in the Coriolis

Matrix that can be computed recursively in an algorithm in terms of composite quantities of the spatial inertia \mathbf{I}_i and the quantity $\mathbf{B}(\mathbf{v}_i, \mathbf{I}_i)$. By taking the derivative of our expressions for \mathbf{C}_{ij} with respect to \dot{q}_k , we found expressions for the Christoffel symbols that are also implementable in a recursive algorithm. Our $O(Nd)$ and $O(Nd^2)$ algorithms to compute the Coriolis Matrix and Christoffel Symbols, respectively, proved to be fast. For 20 DoF biped it took only 18 μs to compute \mathbf{C} and 122 μs for Γ_{ijk} . Due to effects of branching, the algorithms compute faster for a 19 DoF quadruped, where it took only 10 μs for \mathbf{C} and 37 μs for Γ_{ijk} . Given the efficiency, scalability, and speed of these algorithms, we conclude that they are viable for implementation in real-time control loops as well as other dynamics applications.

Acknowledgements

The authors gratefully acknowledge NSF Grant CMMI 1835186 and ONR Award N0001420WX01278 (through a sub-award to Notre Dame) for partial support of this work. The authors thank Gianluca Garafalo and Christian Ott for stimulating discussions underpinning multiple remarks. The authors also gratefully acknowledge Jared Di Carlo for early work and discussions on the algorithm for the Christoffel symbols.

References

- [1] R. Featherstone, *Rigid Body Dynamics Algorithms*. Springer, 2008.
- [2] M. W. Walker and D. E. Orin, “Efficient Dynamic Computer Simulation of Robotic Mechanisms,” *Journal of Dynamic Systems, Measurement, and Control*, vol. 104, no. 3, pp. 205–211, 09 1982.
- [3] Y. Abe, M. da Silva, and J. Popović, “Multiobjective control with frictional contacts,” in *2007 ACM SIGGRAPH/Eurographics Symp. on Computer Animation*, Aire-la-Ville, Switzerland, 2007, pp. 249–258.
- [4] J. Park, J. Haan, and F. Park, “Convex optimization algorithms for active balancing of humanoid robots,” *IEEE Transactions on Robotics*, vol. 23, no. 4, pp. 817–822, Aug. 2007.
- [5] P. M. Wensing and D. E. Orin, “Generation of dynamic humanoid behaviors through task-space control with conic optimization,” in *IEEE Int. Conf. on Rob. and Automation*, May 2013, pp. 3103–3109.
- [6] S. Kuindersma, R. Deits, M. Fallon, A. Valenzuela, H. Dai, F. Permenter, T. Koolen, P. Marion, and R. Tedrake, “Optimization-based locomotion planning, estimation, and control design for the atlas humanoid robot,” *Autonomous Robots*, vol. 40, no. 3, pp. 429–455, 2015.
- [7] A. De Luca and L. Ferrajoli, “A modified newton-euler method for dynamic computations in robot fault detection and control,” in *IEEE International Conference on Robotics and Automation*, May 2009, pp. 3359–3364.
- [8] G. Bledt, P. M. Wensing, S. Ingersoll, and S. Kim, “Contact model fusion for event-based locomotion in unstructured terrains,” in *IEEE International Conference on Robotics and Automation*, 2018, pp. 1–8.
- [9] A. Jain and G. Rodriguez, “Recursive linearization of manipulator dynamics models,” in *IEEE International Conference on Systems, Man and Cybernetics*, nov 1990, pp. 475–480.
- [10] G. A. Sohl and J. E. Bobrow, “A recursive multibody dynamics and sensitivity algorithm for branched kinematic chains,” *Journal of Dynamic Systems, Measurement, and Control*, vol. 123, no. 3, pp. 391–399, 2001.
- [11] A. Jain and G. Rodriguez, “Linearization of manipulator dynamics using spatial operators,” *IEEE Transactions on Systems, Man and Cybernetics*, vol. 23, no. 1, pp. 239–248, jan/feb 1993.
- [12] J. Murray and D. Johnson, “The linearized dynamic robot model: efficient computation and practical applications,” in *IEEE Conference on Decision and Control*, dec 1989, pp. 1659–1664 vol.2.
- [13] J. Bobrow, F. Park, and A. Sideris, *Recent Advances on the Algorithmic Optimization of Robot Motion*. Berlin, Heidelberg: Springer Berlin Heidelberg, 2006, pp. 21–41.
- [14] W. Suleiman, E. Yoshida, J. Laumond, and A. Monin, “Optimizing humanoid motions using recursive dynamics and lie groups,” in *International Conference on Information and Communication Technologies: From Theory to Applications*, April 2008, pp. 1–6.
- [15] H.-C. Lin, T.-C. Lin, and K. Yae, “On the skew-symmetric property of the newton-euler formulation for open-chain robot manipulators,” in *American Control Conference*, vol. 3, June 1995, pp. 2322–2326.
- [16] H. Wang, “On the recursive implementation of adaptive control for robot manipulators,” in *Chinese Control Conference (CCC)*, July 2010, pp. 2154–2161.
- [17] —, “Recursive composite adaptation for robot manipulators,” *Journal of Dynamic Systems, Measurement, and Control*, vol. 135, no. 2, pp. 021 010–021 010, 11 2012.
- [18] M. Safeea, P. Neto, and R. Bearee, “Robot dynamics: A recursive algorithm for efficient calculation of christoffel symbols,” *Mechanism and Machine Theory*, vol. 142, p. 103589, 2019.
- [19] B. Siciliano, L. Sciavicco, L. Villani, and G. Oriolo, *Robotics: modelling, planning and control*. Springer Science & Business Media, 2010.
- [20] J.-J. E. Slotine and W. Li, “On the adaptive control of robot manipulators,” *Int. J. of Robotics Research*, vol. 6, no. 3, pp. 49–59, 1987.
- [21] K. M. Lynch and F. C. Park, *Modern Robotics*. Cambridge University Press, 2017.
- [22] F. Park, J. Bobrow, and S. Ploen, “A lie group formulation of robot dynamics,” *The International Journal of Robotics Research*, vol. 14, no. 6, pp. 609–618, 1995.
- [23] S. Traversaro and A. Saccon, “Multibody dynamics notation,” Technische Universiteit Eindhoven, Tech. Rep., 2016. [Online]. Available: <http://repository.tue.nl/849895>

- [24] G. Niemeyer and J.-J. E. Slotine, "Performance in adaptive manipulator control," *The International Journal of Robotics Research*, vol. 10, no. 2, pp. 149–161, 1991.
- [25] G. Niemeyer and J.-J. Slotine, "Performance in adaptive manipulator control," in *IEEE Conference on Decision and Control*, Dec 1988, pp. 1585–1591 vol.2.
- [26] G. D. Niemeyer, "Computational algorithms for adaptive robot control," Master's thesis, MIT, 1990.
- [27] S. Ploen, "A skew-symmetric form of the recursive newton-euler algorithm for the control of multibody systems," in *American Control Conference*, vol. 6, 1999, pp. 3770–3773 vol.6.
- [28] G. Garofalo, C. Ott, and A. Albu-Schaffer, "On the closed form computation of the dynamic matrices and their differentiations," in *IEEE/RSJ International Conference on Intelligent Robots and Systems*, Nov 2013, pp. 2364–2359.
- [29] T. R. Kane and D. A. Levinson, *Dynamics, theory and applications*. McGraw Hill, 1985.
- [30] G. Garofalo, B. Henze, J. Engelsberger, and C. Ott, "On the inertially decoupled structure of the floating base robot dynamics," *IFAC-PapersOnLine*, vol. 48, no. 1, pp. 322–327, 2015.
- [31] G. Garofalo, F. Beck, and C. Ott, "Task-space tracking control for underactuated aerial manipulators," in *European Control Conference*, 2018, pp. 628–634.
- [32] R. W. Brockett, A. Stokes, and F. Park, "A geometrical formulation of the dynamical equations describing kinematic chains," in *[1993] Proceedings IEEE International Conference on Robotics and Automation*, May 1993, pp. 637–641 vol.2.
- [33] A. Müller and P. Maisser, "A lie-group formulation of kinematics and dynamics of constrained mbs and its application to analytical mechanics," *Multibody system dynamics*, vol. 9, no. 4, pp. 311–352, 2003.
- [34] A. Müller and Z. Terze, "Geometric methods and formulations in computational multibody system dynamics," *Acta Mechanica*, vol. 227, no. 12, pp. 3327–3350, 2016.
- [35] H. Wei, G. Weibing, and C. Mian, "A new robot model and associated control algorithm," *ACTA Automatic Sinica*, vol. 20, no. 3, pp. 278–285, 1994, (in Chinese).
- [36] M. L. Felis, "RBDL: an efficient rigid-body dynamics library using recursive algorithms," *Autonomous Robots*, pp. 1–17, 2016.

Spatial Vectors and Operators in Coordinates

The main body of this paper has predominantly employed coordinate-free expressions to accelerate the development of algorithms. However, for any numerical implementation, all the objects (velocities, inertias, etc.) must be expressed in some basis. This appendix reviews the coordinate representation of spatial vector quantities when a Plücker basis is employed. When working with Cartesian vectors, a coordinate frame provides three unit vectors that serve as a basis for 3D Euclidean space. When working with

spatial vectors, a coordinate frame is also equipped with an origin location in space, and this origin location represents three additional degrees of freedom. The choice of a frame origin and frame orientation together set a Plücker basis [1] for spatial motion vectors as follows.

Any spatial velocity is a 6D vector representing linear and angular 3D velocities such that when expressed in the Plücker basis for the frame attached to body i (frame i),

$${}^i\{\mathbf{v}_i\} = \begin{bmatrix} {}^i\{\boldsymbol{\omega}_i\} \\ {}^i\{\mathbf{v}_i\} \end{bmatrix} \quad (57)$$

where $\boldsymbol{\omega}_i \in \mathbb{R}^3$ and $\mathbf{v}_i \in \mathbb{R}^3$ are the angular velocity of frame i and linear velocity of its coordinate origin. Both Cartesian vectors are expressed using the coordinate axes of frame i .

Similarly, spatial force is defined in terms of the 3D moment and linear force acting on body i so that when expressed in the dual Plücker basis associated with frame i

$${}^i\{\mathbf{f}_i\} = \begin{bmatrix} {}^i\{\mathbf{n}_i\} \\ {}^i\{\mathbf{f}_i\} \end{bmatrix} \quad (58)$$

where \mathbf{n}_i is the moment about the origin of frame i and \mathbf{f}_i is a linear force. Both Cartesian vectors are expressed using the Cartesian basis of frame i .

The expression of spatial vectors can be changed from frame i to frame j using a Spatial Transform Matrix defined as

$${}^j\mathbf{X}_i = \begin{bmatrix} {}^j\mathbf{R}_i & \mathbf{0} \\ -{}^j\mathbf{R}_i\mathbf{S}({}^i\{\mathbf{p}_{j/i}\}) & {}^j\mathbf{R}_i \end{bmatrix}. \quad (59)$$

where ${}^j\mathbf{R}_i \in \mathbb{R}^{3 \times 3}$ is the rotation matrix from frame i to frame j , ${}^i\{\mathbf{p}_{j/i}\} \in \mathbb{R}^3$ is the vector from the origin of frame i to the origin of frame j , and $\mathbf{S}(\{\mathbf{p}\})$ is the skew-symmetric 3D cross product matrix defined for $\{\mathbf{p}\} = [p_x, p_y, p_z]^T \in \mathbb{R}^3$ as

$$\mathbf{S}(\{\mathbf{p}\}) = \begin{bmatrix} 0 & -p_z & p_y \\ p_z & 0 & -p_x \\ -p_y & p_x & 0 \end{bmatrix}. \quad (60)$$

Given any basis for \mathcal{M} , the Spatial Cross Product Matrix is defined for a 6D vector as

$$\{[\mathbf{v} \times]\} = \begin{bmatrix} \mathbf{S}(\{\boldsymbol{\omega}\}) & \mathbf{0} \\ \mathbf{S}(\{\mathbf{v}\}) & \mathbf{S}(\{\boldsymbol{\omega}\}) \end{bmatrix}. \quad (61)$$

in the sense that for any $\mathbf{v}_1, \mathbf{v}_2 \in \mathcal{M}$

$$\{[\mathbf{v}_1 \times]\}\{\mathbf{v}_2\} = \{\mathbf{v}_1 \times \mathbf{v}_2\}$$

as long as both vectors are expressed with the same basis.

In similar fashion we can express the $\bar{\times}^*$ operator as

$$\{\mathbf{f} \bar{\times}^*\} = \begin{bmatrix} -\mathbf{S}(\{\mathbf{n}\}) & -\mathbf{S}(\{\mathbf{f}\}) \\ -\mathbf{S}(\{\mathbf{f}\}) & \mathbf{0} \end{bmatrix}. \quad (62)$$

Using the Plücker basis and its dual associated with frame i , the spatial inertial of body i is expressed in coordinates as

$${}^i\{\mathbf{I}_i\} = \begin{bmatrix} {}^i\{\bar{\mathbf{I}}_i\} & m_i \mathbf{S}({}^i\{\mathbf{c}_i\}) \\ m_i \mathbf{S}({}^i\{\mathbf{c}_i\})^\top & m_i \mathbf{1}_3 \end{bmatrix} \quad (63)$$

where m_i is the mass of body i , ${}^i\{\mathbf{c}_i\} \in \mathbb{R}^3$ is the vector to the center of mass of body i expressed in local coordinates, $\mathbf{1}_3 \in \mathbb{R}^{3 \times 3}$ is the identity matrix, and ${}^i\{\bar{\mathbf{I}}_i\} \in \mathbb{R}^{3 \times 3}$ is the conventional 3D rotational inertial tensor about the coordinate origin with elements

$${}^i\{\bar{\mathbf{I}}_i\} = \begin{bmatrix} I_{xx} & I_{xy} & I_{xz} \\ I_{xy} & I_{yy} & I_{yz} \\ I_{xz} & I_{yz} & I_{zz} \end{bmatrix}. \quad (64)$$

Supplemental Derivation for Equation (19)

Toward simplifying (18), consider the following summation lemma:

Lemma 1. *Let body i with the following set*

$$S(i) = \{(k, j) \mid k \succeq i \text{ and } j \preceq k\}$$

The set can also be represented via:

$$S(i) = \{(k, j) \mid j \sim i \text{ and } k \succeq [ij]\}$$

Proof.

$$\begin{aligned} S(i) &= \{(k, j) \mid k \succeq i \text{ and } j \preceq k\} \\ &= \{(k, j) \mid k \succeq i \text{ and } k \succeq j\} \end{aligned}$$

Noting that it is only possible for $k \succeq i$ and $k \succeq j$ when j and i are related, the sum simplifies as

$$S(i) = \{(k, j) \mid j \sim i \text{ and } k \succeq [ij]\} \quad (65)$$

□

Expanding (18):

$$\boldsymbol{\tau}_i = \sum_{k \succeq i} \boldsymbol{\Phi}_i^\top \mathbf{I}_k \left(\sum_{j \preceq k} \boldsymbol{\Phi}_j \ddot{\mathbf{q}}_j + \dot{\boldsymbol{\Phi}}_j \dot{\mathbf{q}}_j \right) \quad (66)$$

$$+ \boldsymbol{\Phi}_i^\top \mathbf{B}_k \left(\sum_{j \preceq k} \boldsymbol{\Phi}_j \dot{\mathbf{q}}_j \right) \quad (67)$$

$$= \sum_{k \succeq i} \sum_{j \preceq k} \boldsymbol{\Phi}_i^\top \mathbf{I}_k \boldsymbol{\Phi}_j \ddot{\mathbf{q}}_j \quad (68)$$

$$+ \left(\boldsymbol{\Phi}_i^\top \mathbf{I}_k \dot{\boldsymbol{\Phi}}_j + \boldsymbol{\Phi}_i^\top \mathbf{B}_k \boldsymbol{\Phi}_j \right) \dot{\mathbf{q}}_j \quad (69)$$

However, through application of Lemma 1:

$$\boldsymbol{\tau}_i = \sum_{j \sim i} \sum_{k \succeq [ij]} \boldsymbol{\Phi}_i^\top \mathbf{I}_k \boldsymbol{\Phi}_j \ddot{\mathbf{q}}_j + \quad (70)$$

$$+ \left(\boldsymbol{\Phi}_i^\top \mathbf{I}_k \dot{\boldsymbol{\Phi}}_j + \boldsymbol{\Phi}_i^\top \mathbf{B}_k \boldsymbol{\Phi}_j \right) \dot{\mathbf{q}}_j \quad (71)$$

$$= \sum_{j \sim i} \boldsymbol{\Phi}_i^\top \mathbf{I}_{[ij]}^C \boldsymbol{\Phi}_j \ddot{\mathbf{q}}_j + \quad (72)$$

$$\left(\boldsymbol{\Phi}_i^\top \mathbf{I}_{[ij]}^C \dot{\boldsymbol{\Phi}}_j + \boldsymbol{\Phi}_i^\top \mathbf{B}_{[ij]}^C \boldsymbol{\Phi}_j \right) \dot{\mathbf{q}}_j \quad (73)$$

where the composite quantities are defined in the main text.

Proof of Theorem 1

Proof. The transformation law for Christoffel symbols is

$$\bar{\Gamma}_{ijk} = \sum_{\alpha, \beta, \gamma} \frac{\partial q_\alpha}{\partial \bar{q}_i} \frac{\partial q_\beta}{\partial \bar{q}_j} \frac{\partial q_\gamma}{\partial \bar{q}_k} \Gamma_{\alpha\beta\gamma} + \sum_{\alpha, \beta} \frac{\partial^2 q_\alpha}{\partial \bar{q}_j \bar{q}_k} \frac{\partial q_\beta}{\partial \bar{q}_i} H_{\alpha\beta} \quad (74)$$

Multiplying both sides by $\dot{\bar{q}}_k$ and summing over k we have:

$$\begin{aligned} \bar{C}_{ij}^\star &= \sum_{\alpha, \beta, \gamma, k} \frac{\partial q_\alpha}{\partial \bar{q}_i} \frac{\partial q_\beta}{\partial \bar{q}_j} \left(\frac{\partial q_\gamma}{\partial \bar{q}_k} \dot{\bar{q}}_k \right) \Gamma_{\alpha\beta\gamma} + \\ &\quad \sum_{\alpha, \beta} \left(\frac{\partial^2 q_\beta}{\partial \bar{q}_j \bar{q}_k} \dot{\bar{q}}_k \right) \frac{\partial q_\alpha}{\partial \bar{q}_i} H_{\alpha\beta} \\ &= \sum_{\alpha, \beta, \gamma} \frac{\partial q_\alpha}{\partial \bar{q}_i} \frac{\partial q_\beta}{\partial \bar{q}_j} \Gamma_{\alpha\beta\gamma} \dot{q}_\gamma + \sum_{\alpha, \beta} \left(\frac{d}{dt} \frac{\partial q_\beta}{\partial \bar{q}_j} \right) \frac{\partial q_\alpha}{\partial \bar{q}_i} H_{\alpha\beta} \\ &= \sum_{\alpha, \beta} A_{\alpha i} C_{\alpha\beta}^\star A_{\beta j} + A_{\alpha i} H_{\alpha\beta} \dot{A}_{\beta j} \\ &= \left[\mathbf{A}^\top \mathbf{C}^\star \mathbf{A} + \mathbf{A} \mathbf{H} \dot{\mathbf{A}} \right]_{ij} \end{aligned}$$

□